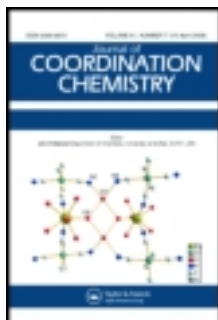


This article was downloaded by: [122.194.31.99]

On: 04 September 2013, At: 22:19

Publisher: Taylor & Francis

Informa Ltd Registered in England and Wales Registered Number: 1072954 Registered office: Mortimer House, 37-41 Mortimer Street, London W1T 3JH, UK



Journal of Coordination Chemistry

Publication details, including instructions for authors and subscription information:

<http://www.tandfonline.com/loi/gcoo20>

Syntheses, structures, and host-guest interactions of 2-D grid-type cyanide-bridged compounds [Zn(L)(H₂O)₂][M(CN)₄]·3H₂O (L = N,N'-bis(4-pyridylformamide)-1,4-benzene; M = Ni, Pd or Pt)

Aiyun Hu^a, Xin Chen^a, Hu Zhou^{bc}, Yingying Chen^a & Aihua Yuan^a

^a School of Biology and Chemistry Engineering, Jiangsu University of Science and Technology, Zhenjiang, P.R. China

^b School of Material Science and Engineering, Jiangsu University of Science and Technology, Zhenjiang, P.R. China

^c SiYang Diesel Engine Manufacturing Co., Ltd, Zhenjiang, P.R. China

Accepted author version posted online: 07 Aug 2013. Published online: 02 Sep 2013.

To cite this article: Aiyun Hu, Xin Chen, Hu Zhou, Yingying Chen & Aihua Yuan (2013) Syntheses, structures, and host-guest interactions of 2-D grid-type cyanide-bridged compounds [Zn(L)(H₂O)₂][M(CN)₄]·3H₂O (L = N,N'-bis(4-pyridylformamide)-1,4-benzene; M = Ni, Pd or Pt), Journal of Coordination Chemistry, 66:18, 3241-3248, DOI: [10.1080/00958972.2013.832229](https://doi.org/10.1080/00958972.2013.832229)

To link to this article: <http://dx.doi.org/10.1080/00958972.2013.832229>

PLEASE SCROLL DOWN FOR ARTICLE

Taylor & Francis makes every effort to ensure the accuracy of all the information (the "Content") contained in the publications on our platform. However, Taylor & Francis, our agents, and our licensors make no representations or warranties whatsoever as to the accuracy, completeness, or suitability for any purpose of the Content. Any opinions and views expressed in this publication are the opinions and views of the authors, and are not the views of or endorsed by Taylor & Francis. The accuracy of the Content should not be relied upon and should be independently verified with primary sources of information. Taylor and Francis shall not be liable for any losses, actions, claims, proceedings, demands, costs, expenses, damages, and other liabilities whatsoever or

howsoever caused arising directly or indirectly in connection with, in relation to or arising out of the use of the Content.

This article may be used for research, teaching, and private study purposes. Any substantial or systematic reproduction, redistribution, reselling, loan, sub-licensing, systematic supply, or distribution in any form to anyone is expressly forbidden. Terms & Conditions of access and use can be found at <http://www.tandfonline.com/page/terms-and-conditions>

Syntheses, structures, and host-guest interactions of 2-D grid-type cyanide-bridged compounds $[\text{Zn}(\text{L})(\text{H}_2\text{O})_2][\text{M}(\text{CN})_4] \cdot 3\text{H}_2\text{O}$ ($\text{L} = N,N'$ -bis(4-pyridylformamide)-1,4-benzene; $\text{M} = \text{Ni}, \text{Pd}$ or Pt)

AIYUN HU[†], XIN CHEN[†], HU ZHOU^{‡§}, YINGYING CHEN[†] and AIHUA YUAN^{*†}

[†]School of Biology and Chemistry Engineering, Jiangsu University of Science and Technology, Zhenjiang, P.R. China

[‡]School of Material Science and Engineering, Jiangsu University of Science and Technology, Zhenjiang, P.R. China

[§]SiYang Diesel Engine Manufacturing Co., Ltd, Zhenjiang, P.R. China

(Received 20 March 2013; accepted 19 July 2013)

Self-assembly of Zn^{2+} , the pillar ligand N,N' -bis(4-pyridylformamide)-1,4-benzene, and $[\text{M}(\text{CN})_4]^{2-}$ ($\text{M} = \text{Ni}, \text{Pd},$ or Pt) formed three compounds $[\text{Zn}(\text{L})(\text{H}_2\text{O})_2][\text{M}(\text{CN})_4] \cdot 3\text{H}_2\text{O}$ (**1–3**). Single-crystal X-ray diffraction (XRD) analysis reveals that **1–3** are isostructural and consist of cyanide-bridged 2-D grid-type layers built of $[\text{Zn}(\text{L})(\text{H}_2\text{O})_2]^{2+}$ chains cross-linked by $[\text{M}(\text{CN})_4]^{2-}$ units. Thermogravimetric and powder XRD analyses indicate that **1** has a high thermal stability and exhibits reversibility for desorption/resorption of water guest molecules.

Keywords: Tetracyanometalates; Structures; Grid; Host-guest

1. Introduction

The design and synthesis of functional coordination compounds have grown rapidly because of their intriguing topologies and potential applications [1, 2]. Tetracyanide-bearing precursors $[\text{M}(\text{CN})_4]^{2-}$ ($\text{M} = \text{Ni}, \text{Pd}$ or Pt) were used to construct Hofmann-type host compounds formulated as $\text{ML}_2 \text{M}'(\text{CN})_4$ ($\text{M} = \text{Mn}, \text{Fe}, \text{Co}, \text{Ni}, \text{Cu}, \text{Zn},$ or Cd ; $\text{M}' = \text{Ni}, \text{Pd},$ or Pt ; $\text{L} =$ unidentate ligand) and the resulting materials exhibited interesting properties such as spin-crossover and gas storage [3–7]. However, there is still much to be explored in the crystal engineering of 3-D porous Hofmann-type and analogous structures.

As part of our ongoing efforts in construction of new structural types of tetracyanide-based compounds [8, 9], we employed tetracyanometalates as building blocks to react with Zn^{2+} and the linear bidentate ligand N,N' -bis(4-pyridylformamide)-1,4-benzene (L) to obtain 3-D Hofmann-type compounds, in which the metal cyanide layers are pillared by L . Unexpectedly, three isostructural 2-D grid-type compounds $[\text{Zn}(\text{L})(\text{H}_2\text{O})_2][\text{M}(\text{CN})_4] \cdot 3\text{H}_2\text{O}$ ($\text{M} = \text{Ni}$ (**1**), Pd (**2**) or Pt (**3**)) were obtained instead. Failure of the reactions may be attributed

*Corresponding author. Email: aihuyuan@163.com

to the use of the longer linear ligand L. Shorter linear diaza ligands such as pyrazine, 4,4'-bipyridine, 4,4'-dipyridylacetylene, 1,2-bis(4-pyridyl)ethylene, or 1,2-di(4-pyridyl)ethane were usually employed to construct 3-D Hofmann-type materials [6, 10]. In the present contribution, we report the syntheses, crystal structures, thermal stabilities, and host-guest interactions.

2. Experimental

2.1. Materials and methods

All chemicals and solvents were purchased from commercial sources and used as received. *N,N'*-bis(4-pyridylformamide)-1,4-benzene was synthesized according to the method described [11]. IR spectra were measured on a Nicolet FT 1703X spectrophotometer in the form of KBr pellets from 4000–400 cm^{-1} . Powder X-ray diffraction (XRD) patterns were collected with $\text{Cu-K}\alpha$ radiation using a Shimadzu XRD-6000 diffractometer. Thermogravimetric (TG) analyzes were carried out at a ramp rate of 5 $^{\circ}\text{C min}^{-1}$ under N_2 using a Pyris Diamond TGA analyzer.

2.2. Syntheses

Single crystals of **1–3** were prepared at room temperature by slow diffusion of a $\text{CH}_3\text{CN}/\text{H}_2\text{O}$ (1/1) solution (2 mL) containing $\text{ZnSO}_4 \cdot 7\text{H}_2\text{O}$ (0.05 mM) and L (0.05 mM) into a $\text{CH}_3\text{CN}/\text{H}_2\text{O}$ (1/1) solution (20 mL) of $\text{K}_2\text{M}(\text{CN})_4$ (M = Ni, Pd or Pt) (0.05 mM). Yellow block-shaped crystals were obtained after four weeks. Anal. Calcd for $\text{C}_{22}\text{H}_{24}\text{ZnN}_8\text{NiO}_7$ (**1**) (%): C, 41.51; H, 3.80; N, 17.60. Found: C, 41.39; H, 3.76; N, 17.77. IR (KBr, cm^{-1}) for compound **1**: $\nu_{\text{C-N(amide)}} = 1406, 1417 \text{ cm}^{-1}$, $\nu_{\text{C}\equiv\text{N(terminal)}} = 2131 \text{ cm}^{-1}$, $\nu_{\text{C}\equiv\text{N(bridged)}} = 2173 \text{ cm}^{-1}$; for compound **2**: $\nu_{\text{C-N(amide)}} = 1405, 1416 \text{ cm}^{-1}$, $\nu_{\text{C}\equiv\text{N(terminal)}} = 2145 \text{ cm}^{-1}$, $\nu_{\text{C}\equiv\text{N(bridged)}} = 2187 \text{ cm}^{-1}$; for compound **3**: $\nu_{\text{C-N(amide)}} = 1404, 1416 \text{ cm}^{-1}$, $\nu_{\text{C}\equiv\text{N(terminal)}} = 2145 \text{ cm}^{-1}$, $\nu_{\text{C}\equiv\text{N(bridged)}} = 2191 \text{ cm}^{-1}$.

2.3. Crystallographic data collection and structure determination

Diffraction data for **1–3** were collected at 296(3) K on a Bruker Smart APEX II diffractometer equipped with $\text{Mo-K}\alpha$ ($\lambda = 0.71073 \text{ \AA}$) radiation. Diffraction data analysis and reduction were performed within *SMART*, *SAINT* and *XPREP* [12]. Correction for Lorentz, polarization, and absorption effects were performed within *SADABS* [13]. Structures were solved using the Patterson method within *SHELXS-97* and refined using *SHELXL-97* [14,15]. All non-hydrogen atoms were refined with anisotropic thermal parameters. Hydrogens of L were calculated at idealized positions and included in the refinement in a riding mode with U_{iso} for H assigned as 1.2 times U_{eq} of the attached atoms. Hydrogens bound to coordinated and uncoordinated water were located from difference Fourier maps and refined as riding with $U_{\text{iso}}(\text{H}) = 1.2 U_{\text{eq}}(\text{O})$. The crystallographic data and experimental detail for structural analyzes are summarized in table 1. Selected bond distances and angles are listed in table 2.

Table 1. Crystallographic data and structural refinement for 1–3.

Compounds	1	2	3
Formula	C ₂₂ H ₂₄ ZnN ₈ NiO ₇	C ₂₂ H ₂₄ ZnN ₈ PdO ₇	C ₂₂ H ₂₄ ZnN ₈ PtO ₇
<i>M_r</i>	636.60	684.26	772.95
Crystal system	Triclinic	Triclinic	Triclinic
Space group	<i>P</i> -1	<i>P</i> -1	<i>P</i> -1
<i>a</i> (Å)	8.6236(13)	8.623(3)	8.5127(9)
<i>b</i> (Å)	9.9335(15)	10.023(4)	9.9215(10)
<i>c</i> (Å)	17.025(3)	17.138(7)	17.1690(18)
<i>α</i> (°)	85.637(2)	85.869(5)	85.8380(10)
<i>β</i> (°)	82.101(2)	82.515(5)	82.2710(10)
<i>γ</i> (°)	65.338(2)	66.591(5)	67.5370(10)
<i>V</i> (Å ³)	1312.5(3)	1347.4(9)	1327.5(2)
<i>Z</i>	2	2	2
<i>ρ</i> _{Calcd} (g cm ⁻³)	1.611	1.687	1.934
<i>μ</i> (mm ⁻¹)	1.689	1.614	6.224
Total, unique	11,352, 5897	11,646, 6017	9335, 4494
Observed [<i>I</i> > 2σ(<i>I</i>)]	3719	4129	4314
GOF on <i>F</i> ²	0.998	1.012	1.059
<i>R</i> ₁ , ω <i>R</i> ₂ [<i>I</i> > 2σ(<i>I</i>)]	0.0321, 0.0734	0.0346, 0.0737	0.0281, 0.0748
<i>R</i> ₁ , ω <i>R</i> ₂ (all data)	0.0684, 0.0889	0.0663, 0.0870	0.0293, 0.0767

Table 2. Selected bond distances (Å) and angles (°) for 1–3.

1			
Ni1–C1	1.857(3)	N4–C4	1.146(3)
Ni1–C2	1.877(3)	Zn1–N1	2.053(2)
Ni1–C3	1.853(2)	Zn1–N3 ⁱ	2.046(2)
Ni1–C4	1.888(3)	Zn1–N5	2.231(2)
N1–C1	1.143(3)	Zn1–N8 ⁱⁱ	2.223(2)
N2–C2	1.145(3)	Zn1–O1	2.1899(19)
N3–C3	1.145(3)	Zn1–O2	2.2262(19)
N1–C1–Ni1	177.2(3)	N4–C4–Ni1	178.1(3)
N2–C2–Ni1	178.8(3)	C1–N1–Zn1	175.9(2)
N3–C3–Ni1	179.8(3)	C3–N3–Zn1 ⁱⁱⁱ	172.0(2)
2			
Pd1–C1	1.979(3)	N4–C4	1.146(4)
Pd1–C2	2.002(3)	Zn1–N1	2.037(3)
Pd1–C3	1.976(3)	Zn1–N3 ⁱ	2.042(3)
Pd1–C4	2.011(3)	Zn1–N5	2.249(3)
N1–C1	1.142(4)	Zn1–N8 ⁱⁱ	2.236(3)
N2–C2	1.143(4)	Zn1–O1	2.197(2)
N3–C3	1.145(4)	Zn1–O2	2.226(2)
N1–C1–Pd1	178.0(3)	N4–C4–Pd1	178.1(3)
N2–C2–Pd1	178.5(3)	C1–N1–Zn1	174.1(2)
N3–C3–Pd1	177.8(3)	C3–N3–Zn1 ⁱⁱⁱ	175.3(3)
3			
Pt1–C1	1.983(5)	N4–C4	1.148(7)
Pt1–C2	2.012(5)	Zn1–N1	2.033(4)
Pt1–C3	1.980(5)	Zn1–N3 ⁱ	2.047(4)
Pt1–C4	2.007(5)	Zn1–N5	2.248(4)
N1–C1	1.149(7)	Zn1–N8 ⁱⁱ	2.232(4)
N2–C2	1.147(6)	Zn1–O1	2.198(3)
N3–C3	1.144(7)	Zn1–O2	2.212(3)
N1–C1–Pt1	178.3(4)	N4–C4–Pt1	178.7(4)
N2–C2–Pt1	178.8(4)	C1–N1–Zn1	172.9(4)
N3–C3–Pt1	177.9(4)	C3–N3–Zn1 ⁱⁱⁱ	174.3(4)

Symmetry codes for 1: (i) $x-1, y+1, z$; (ii) $x-1, y, z-1$; (iii) $x+1, y-1, z$. for 2: (i) $x+1, y-1, z$; (ii) $x-1, y, z-1$; (iii) $x-1, y+1, z$. for 3: (i) $x-1, y+1, z$; (ii) $x+1, y, z+1$; (iii) $x+1, y-1, z$.

3. Results and discussion

Single-crystal XRD analysis revealed that **1–3** are isostructural and crystallize in the triclinic space group *P*-1 (table 1). Only the structure of **1** is described in detail (figure 1). The asymmetric unit consists of one $[\text{Zn}(\text{L})(\text{H}_2\text{O})_2]^{2+}$, one $[\text{Ni}(\text{CN})_4]^{2-}$, and three crystallization waters. In the $[\text{Zn}(\text{L})(\text{H}_2\text{O})_2]^{2+}$ fragment, the six-coordinate Zn is located in a distorted octahedral geometry, in which the average value (2.277 Å) of Zn–N_L ligand bond distances is larger than 2.050 Å of Zn–N_{cyanide} bonds. Zn1–O1 and Zn1–O2 lengths are 2.1899(19) and 2.2262(19) Å, respectively, while the two Zn–NC bonds are bent slightly with angles of 172.0(2) and 175.9(2)°. The $\{\text{ZnN}_4\text{O}_2\}$ coordination geometry of Zn in our case has also been observed in $\text{Zn}(\text{DMF})_2 \text{M}(\text{CN})_4$ (M = Ni, Pd or Pt) [16]. As a result, $[\text{Zn}(\text{L})(\text{H}_2\text{O})_2]^{2+}$ units are connected alternately through *trans* L to form 2,2-chains with the intrachain Zn···Zn distance of *ca.* 20.11 Å.

$[\text{Ni}(\text{CN})_4]$ exhibits a square planar geometry with four bridging cyanides. The average Ni–C and C–N bond distances are 1.868 and 1.145 Å, respectively, and Ni–CN bonds are nearly linear (177.2(3)–179.8(3)°). The metric parameters of $[\text{Ni}(\text{CN})_4]$ are typical for tetracyanometalates [17–20]. As shown in figure 2, adjacent $[\text{Zn}(\text{L})(\text{H}_2\text{O})_2]^{2+}$ chains are further cross-linked by $[\text{Ni}(\text{CN})_4]^{2-}$, generating a 2-D grid-like network with the two side lengths of about 10.08 and 20.11 Å (Zn···Zn distance). The *trans* coordinated waters are located on both sides of layers. Terminal cyanides, L, coordinated and uncoordinated waters are all involved in the hydrogen-bonding network of **1**. There are four types of hydrogen bonds (table 3): (1) two terminal cyanides interact with coordinated and crystallization waters through O–H···N hydrogen bonds; (2) coordinated waters interact with lattice waters and L by O–H···O hydrogen bonds; (3) lattice waters interact with coordinated/lattice waters and L by O–H···O hydrogen bonds; and (4) L interacts with coordinated and uncoordinated waters by N–H···O hydrogen bonds. As a result, neighboring layers are well separated through hydrogen bonds and π – π stacking interactions, forming a 3-D supramolecular network (figure 3). According to Cheetham [21], cyanide-based systems can be classified using I^xO^y

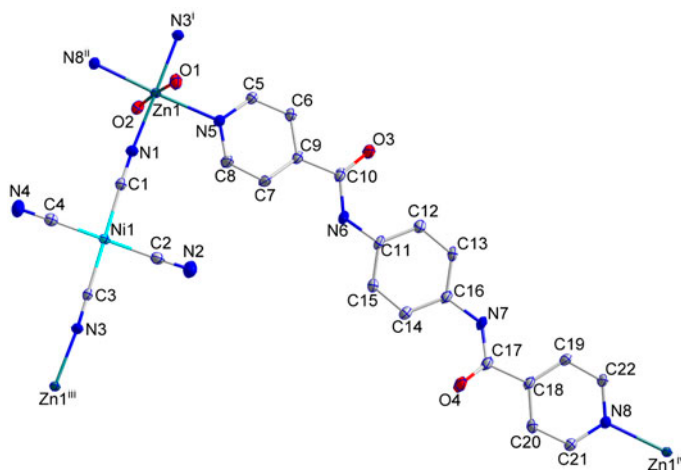


Figure 1. ORTEP of **1** with displacement ellipsoids drawn at the 30% probability level. All hydrogens and crystallization waters were omitted for clarity. Symmetry codes: (i) $x - 1, y + 1, z$; (ii) $x - 1, y, z - 1$; (iii) $x + 1, y - 1, z$; (iv) $x + 1, y, z + 1$.

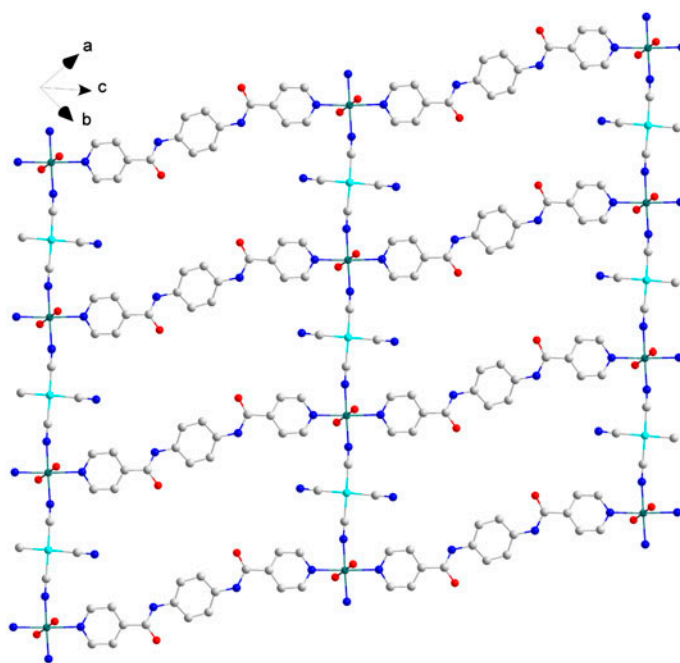


Figure 2. The 2-D grid-type structure of **1**. All hydrogens and crystallization waters were omitted for clarity.

Table 3. Hydrogen-bond geometry (Å, °) for **1**.

<i>D</i> -H... <i>A</i>	<i>D</i> -H	H... <i>A</i>	<i>D</i> ... <i>A</i>	<i>D</i> -H... <i>A</i>
O1-H1A...O4 ^v	0.85	1.94	2.739(2)	156
O1-H1B...O6 ^{vi}	0.85	2.01	2.855(3)	178
O2-H2A...O7	0.85	1.95	2.793(3)	169
O2-H2B...N4 ^{vii}	0.85	1.98	2.831(3)	176
O5-H5A...O6 ⁱⁱⁱ	0.85	2.16	2.982(3)	162
O5-H5B...N2	0.85	2.00	2.828(3)	164
O6-H6A...O3	0.85	1.97	2.819(3)	175
O6-H6B...O5 ^{viii}	0.85	1.98	2.830(3)	175
O7-H7A...O1 ^{ix}	0.85	2.32	3.020(3)	140
O7-H7B...O4 ^x	0.85	2.55	3.137(3)	127
N7-H7C...O2 ^{viii}	0.86	2.37	3.205(3)	163
N6-H6C...O5	0.86	2.47	3.290(3)	161

Symmetry codes: (v) $-x + 2, -y + 1, -z + 1$; (vi) $-x + 1, -y + 2, -z + 1$; (vii) $-x + 2, -y + 1, -z$; (iii) $x + 1, y - 1, z$; (viii) $-x + 2, -y + 2, -z + 1$; (ix) $x + 1, y, z$; (x) $-x + 3, -y + 1, -z + 1$.

symbols, where x and y denoted the dimensionality of the inorganic (I) and organic (O) subnetworks, respectively. In the structures of **1–3**, both the inorganic (-Zn-NC-M- linkages) and organic (-L-Zn-L- linkages) subnetworks are 1-D, so the topology can be described as I^1O^1 . From the perspective of topology, the structure in our case is different obviously from those found in 2-D Hofmann-type materials $M(\text{DMF})_2[\text{M}'(\text{CN})_4]$ ($M = \text{Zn}, \text{Cu}$; $\text{M}' = \text{Ni}, \text{Pd}$ or Pt) and $M(\text{H}_2\text{O})_2[\text{Ni}(\text{CN})_4] \cdot x\text{H}_2\text{O}$ ($M = \text{Mn}, \text{Fe}, \text{Co}, \text{Ni}$ or Cd) with I^2O^0 topology, in which the layers were constructed by cyanide-bridged polymeric 2-D skeletons (inorganic subnetwork) with monodentate ligands on both sides [16, 22–25].

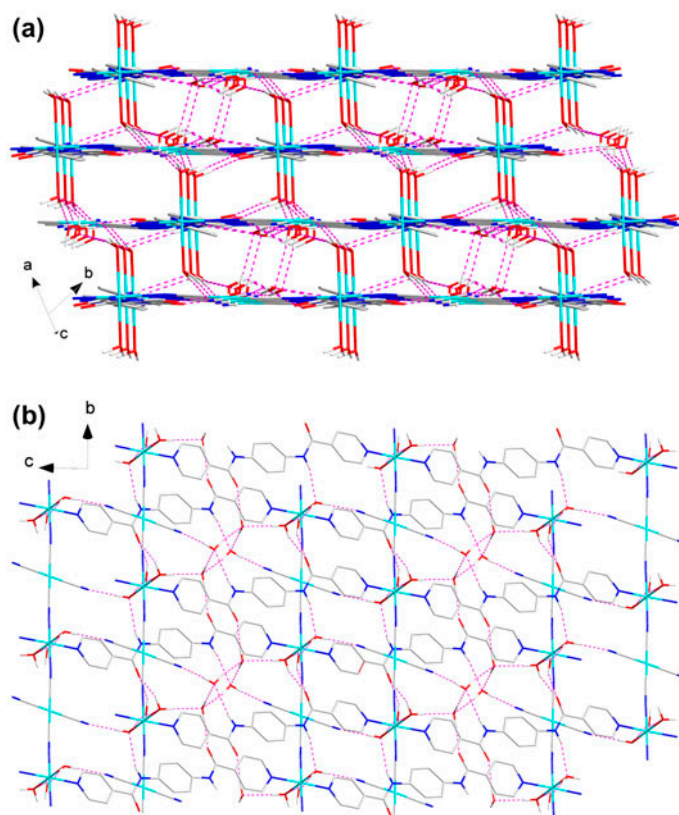


Figure 3. The 3-D supramolecular network of **1** along the (a) [1 0 1] and (b) [1 0 0] directions. All hydrogens bound to carbon were omitted for clarity and dashed lines represent hydrogen bonds.

Taking into account the high price of starting precursors $\text{K}_2\text{Pd}(\text{CN})_4$ and $\text{K}_2\text{Pt}(\text{CN})_4$, only the thermal stability and host-guest chemistry of **1** were investigated. TG curve (Supplementary material) showed an obvious weight loss (13.80%) between 20 and 110 °C, corresponding to loss of three uncoordinated and two coordinated waters per formula unit (Calcd 14.15%). The desolvated phase $\text{Zn}(\text{L})\text{M}(\text{CN})_4$ loses no further mass up to 300 °C, above which thermal decomposition occurs.

Crystal samples of **1** were heated at 150 °C under vacuum for 12 h to remove all water molecules and examine the host-guest chemistry. Powder XRD results (figure 4) showed that the compound remained highly crystalline upon removal of crystallized and coordinated water molecules, although the structure of dehydrated phase of **1** has changed, as evidenced by variable diffraction peaks. A potentially very attractive aspect of this system is that the desorption of guest molecules yielded materials with accessible, exposed coordinatively-unsaturated Zn^{2+} metal sites [26]. In fact, powder XRD patterns of the regenerated samples exhibit peak positions and intensities fully coincident to those observed for as-synthesized samples when dehydrated samples were soaked into water solution over a period of 12 h. Above results indicate that the dehydration/rehydration process of **1** is reversible and removal of water does not result in collapse of the 2-D framework.

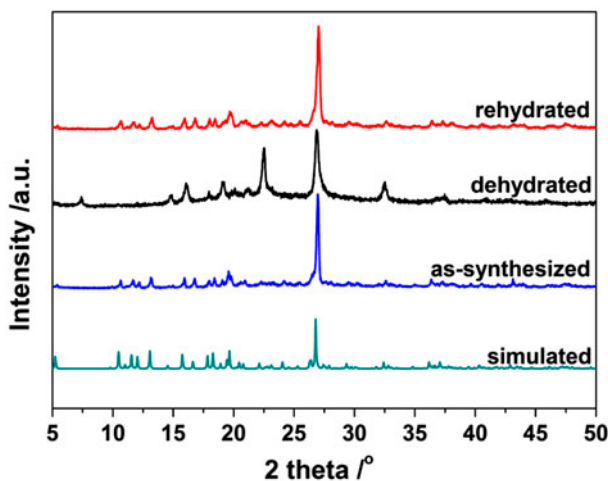


Figure 4. Powder XRD patterns of **1** with the dehydration/rehydration process.

4. Conclusion

Three 2-D grid-type tetracyanide-based compounds were synthesized and characterized structurally. The thermal decomposition and host-guest interaction results reveal that the dehydrated crystals are able to be rehydrated. Continuing work in our laboratory will focus on (1) investigating interactions between the host lattice of dehydrated compounds and other small guest molecules (ethanol, methanol, amine, DMF, etc.) and (2) employing 2-D dehydrated phases as precursors to react with pillar bidentate ligands to construct 3-D porous frameworks with gas storage properties.

Supplementary material

CCDC numbers: 925708 (**1**), 925709 (**2**) and 925710 (**3**). This data can be obtained free of charge from the Cambridge Crystallographic Data Center via www.ccdc.cam.ac.uk/data_request/cif.

Acknowledgments

This research was supported by the projects of National Natural Science Foundation (51072072, 51102119, 51272095), Natural Science Foundation of Jiangsu Province (BK2011518).

References

- [1] H.C. Zhou, J.F. Long, O.M. Yaghi. *Chem. Rev.*, **112**, 673 (2012).
- [2] S.T. Meeck, J.A. Greathouse, M.D. Allendorf. *Adv. Mater.*, **23**, 249 (2011).
- [3] N.F. Sciortino, K.R. Scherl-Gruenwald, G. Chastanet, G.J. Halder, K.W. Chapman, J.F. Létard, C.J. Kepert. *Angew. Chem. Int. Ed.*, **51**, 10154 (2012).
- [4] C. Bartual-Murgui, L. Salmon, A. Akou, N.A. Ortega-Villar, H.J. Shepherd, M.C. Muñoz, G. Molnár, J.A. Real, A. Bousseksou. *Chem. Eur. J.*, **18**, 507 (2012).

- [5] P.D. Southon, L. Liu, E.A. Fellows, D.J. Price, G.J. Halder, K.W. Chapman, B. Moubaraki, K.S. Murray, J.F. Létard, C.J. Kepert. *J. Am. Chem. Soc.*, **131**, 10998 (2009).
- [6] J.T. Culp, M.R. Smith, E. Bittner, B. Bockrath. *J. Am. Chem. Soc.*, **130**, 12427 (2008).
- [7] G. Agusti, S. Cobo, A.B. Gaspar, G. Molnár, N.O. Moussa, P.A. Szilágyi, V. Pálfi, C. Vieu, M.C. Muñoz, J.A. Real, A. Bousseksou. *Chem. Mater.*, **20**, 6721 (2008).
- [8] X. Chen, H. Zhou, Y.Y. Chen, A.H. Yuan. *CrystEngComm*, **13**, 5666 (2011).
- [9] A.H. Yuan, R.Q. Lu, H. Zhou, Y.Y. Chen, Y.Z. Li. *CrystEngComm*, **12**, 1382 (2010).
- [10] J.T. Culp, S. Natesakhawat, M.R. Smith, E. Bittner, C. Matranga, B. Bockrath. *J. Phys. Chem.*, **C112**, 7079 (2008).
- [11] L. Song, W.X. Chai, J.W. Lan. *Acta Crystallogr.*, **E65**, 1749 (2009).
- [12] Bruker. *SMART, SAINT and XPREP: Area Detector Control and Data Integration and Reduction Software*, Bruker Analytical X-ray Instruments Inc., Madison, Wisconsin, USA (1995).
- [13] G.M. Sheldrick. *SADABS: Empirical Absorption and Correction Software*, University of Göttingen, Göttingen, Germany (1996).
- [14] G.M. Sheldrick, *SHELXS-97, Program for X-ray Crystal Structure Determination*, University of Göttingen, Göttingen, Germany (1997).
- [15] G.M. Sheldrick. *Acta Crystallogr.*, **A64**, 112 (2008).
- [16] R.Q. Lu, H. Zhou, Y.Y. Chen, J. Xiao, A.H. Yuan. *J. Coord. Chem.*, **63**, 794 (2010).
- [17] J.T. Culp, C. Madden, K. Kauffman, F. Shi, C. Matranga. *Inorg. Chem.*, **52**, 4205 (2013).
- [18] J. Xia, T.T. Li, X.Q. Zhao, J.F. Wei. *J. Coord. Chem.*, **66**, 539 (2013).
- [19] A.H. Hu, X. Chen, Y.Y. Chen, H. Zhou, A.H. Yuan. *J. Mol. Struct.*, **1037**, 301 (2013).
- [20] A. Karadağ, Ş.A. Korkmaz, Ö. Andaç, Y. Yerli, Y. Topcu. *J. Coord. Chem.*, **65**, 1685 (2012).
- [21] A.K. Cheetham, C.N.R. Rao, R.K. Feller. *Chem. Commun.*, **4780**, (2006).
- [22] R.Q. Lu, Y.Y. Chen, H. Zhou, A.H. Yuan. *Acta Chim. Sinica.*, **68**, 1199 (2010).
- [23] R.Q. Lu, H. Zhou, A.H. Yuan. *Chin., J. Inorg. Chem.*, **26**, 347 (2010).
- [24] G.S. Kürkçüoğlu, O.Z. Yeşilel, İ. Kavlak, O. Büyükgüngör. *Struct. Chem.*, **19**, 879 (2008).
- [25] E. Ruiz, S. Alvarez. *Inorg. Chem.*, **34**, 3260 (1995).
- [26] M. Dinca, J.R. Long. *Angew. Chem. Int. Ed.*, **47**, 6766 (2008).